



FE simulation of soft wing impactor for aviation mast frangibility testing – sensitivity to model assumptions

Terje Rølvåg, Torgeir Welo, Rien van Houten & Jaap Wiggenraad

To cite this article: Terje Rølvåg, Torgeir Welo, Rien van Houten & Jaap Wiggenraad (2016): FE simulation of soft wing impactor for aviation mast frangibility testing – sensitivity to model assumptions, International Journal of Crashworthiness, DOI: [10.1080/13588265.2016.1168609](https://doi.org/10.1080/13588265.2016.1168609)

To link to this article: <http://dx.doi.org/10.1080/13588265.2016.1168609>



Published online: 22 Apr 2016.



Submit your article to this journal [↗](#)



Article views: 9



View related articles [↗](#)



View Crossmark data [↗](#)

FE simulation of soft wing impactor for aviation mast frangibility testing – sensitivity to model assumptions

Terje Rølvåg ^a, Torgeir Welo ^a, Rien van Houten^a and Jaap Wiggenraad^b

^aDepartment of Engineering Design and Materials, NTNU, Trondheim, Norway; ^bNational Aerospace Laboratory, Marknesse, The Netherlands

ABSTRACT

In 1981, the International Civil Aviation Organization (ICAO) instigated the 'Frangible Aids Study Group' (FASG), with the aim to define design requirements and crash test procedures addressing the frangibility of airport navigation aids and their support masts. The FASG group soon stated that a specific wing section model should be used as a standard test impactor. This paper describes an attempt to model and verify a virtual model of a wing impactor based on static and dynamic compression test sensitivity analyses. The motivation is to define a standard FE model that will ultimately reduce the need for physical testing, while providing improved opportunities for understanding mechanisms and design parameters related to frangibility. The sensitivity to finite element (FE) model assumptions is studied to ensure a representative deflection-force characteristic for crash tests. The study shows that strain at a fracture value of 15% combined with a bi-linear hardening model gives the most reliable simulation results. This material combination also seems to give the most correct wing impactor behaviour in high-speed crash simulations. The simulations also prove that 1 kHz low pass filtering of reaction forces efficiently eliminates artificial peak forces not contributing to wing damage.

ARTICLE HISTORY

Received 25 June 2015
Accepted 11 March 2016

KEYWORDS

Frangibility; aviation mast; wing impactor; sensitivity; material models; crash simulation

1. Introduction

In 1981, the International Civil Aviation Organization (ICAO) instigated the 'Frangible Aids Study Group' (FASG), with the aim to develop design requirements and crash test procedures addressing the necessary frangibility of airport navigation aids and their support masts. First, the FASG defined that any structure required to be frangible, should break, distort or yield readily when subjected to the sudden collision forces of a 3000-kg aircraft airborne, and travelling in any direction at 140 km/h (75 kt). Subsequently, the FASG determined that frangibility should be demonstrated by conducting full-scale impact tests of these structures. The FASG soon thereupon stated that a specific wing section should be used as a standard test impactor.

Various manufacturers developed, or had already developed approach light structures (ALS) with intended frangible properties, and submitted those to full-scale testing. These tests implied running a soft wing impactor at 140 km/h against the ALS, and assessing its failure mode. 'Soft' representative wing sections were used as impactor, so the amount of damage to the wing section as the result of the collision with the ALS would provide an indication of the frangibility of the ALS.

A 'soft' wing impactor, developed and used for testing by the Netherlands' National Aerospace Laboratory (NLR) in 1988, was used for physical testing of Finnish, Swedish and Norwegian ALS masts between 1991 and 1997. During the period 1998–2000, Canadian ALS masts were tested with a slightly different soft wing impactor, as well as with a rigid impactor (steel tube). Based upon the results of the test campaigns for wing section impacts on five different ALS support structures, design requirements for frangible structures were defined. A maximum peak force on the wing, and a maximum energy absorbed by the wing section, as the result from an impact with the navigation aid and its support structure, were proposed as the critical design criteria for the frangibility of the structure (Figure 1).

However, the ICAO standard [9] as published in 2006, resulting from the work of the FASG, recommends the use of rigid impactors for testing, based on the arguments given by Zimcik et al. in 2004 [21]. Zimcik's physical test results obtained for the Canadian masts show that in comparison to soft wing impactors, rigid impactors provide conservative and repeatable results, and at reduced costs due to the potential for reuse of rigid impactors in physical tests. The reported initial peak

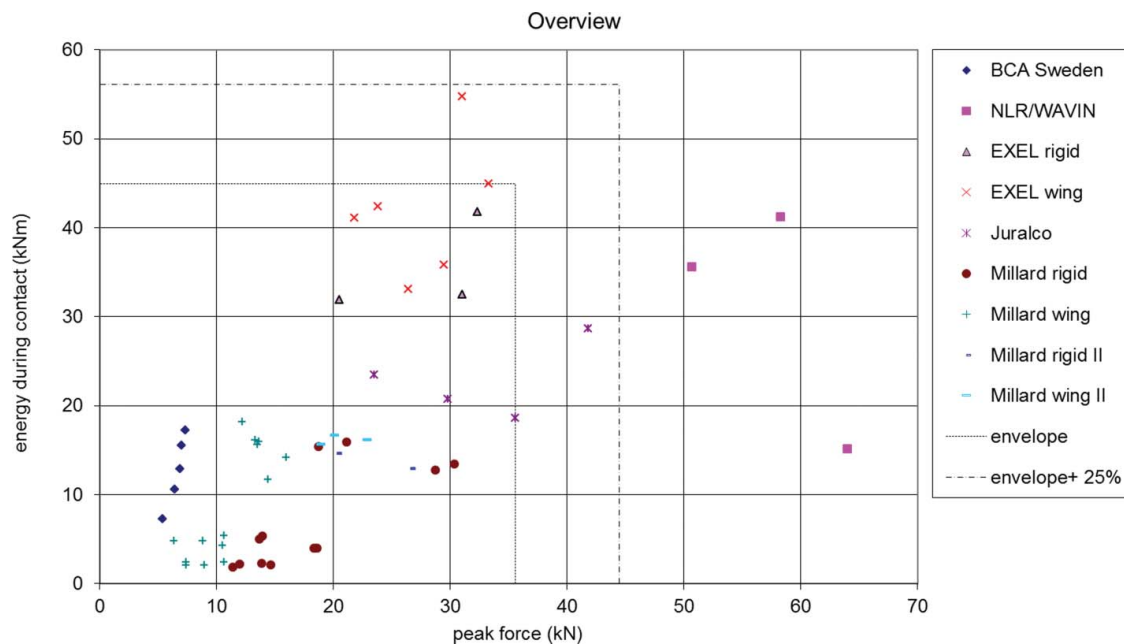


Figure 1. Physical crash test results used to define the ICAO standard.

load and the accumulated energy were within the design criteria for frangibility formulated, and demonstrated that the tested mast was frangible and met the ICAO standard with good margins, even when using a rigid impactor.

With the exception of crash experiments at NLR [17] and at MIRA, presented at the 2014 JAFSG [10] meeting by Griffith [7], very few physical tests have been reported after 2000. Instead of using a soft wing impactor, Griffith used a 'rigid' impactor as proposed in the ICAO standard [9]. His results were dominated by noise due to resonance problems and the author, therefore, recommended using a deformable soft impactor in future tests, rather than a rigid impactor. Similar resonance problems were observed and reported in virtual and physical tests by Rølvåg [15] and Dan Duke [4], among others.

M.H. van Houten et al. [17] identified the difference in impacts by a rigid impactor and impacts by a soft wing impactor. The structure of the soft wing impactor developed by NLR is based on the wing structure of a Beechcraft Model 80 Queen Air, which has an aircraft weight of approximately 3 tons, while the ICAO prescribes a rigid impactor as a thick-walled, semi-circular steel tube, without reference to any particular aircraft. Both rigid and soft impactors are meant to hit the mast at a speed of 140 km/h [9]. The main difference is the initial peak force that occurs when an impactor with a 25-mm thick steel front plate versus a 0.8 mm aluminium sheet structure hits rigid components like the hinges on an aviation mast. In tests [18], the initial peak force at first impact is not always the highest, and a higher one

may occur later in the impact sequence depending on the layout of the mast. Simulation results obtained by Rølvåg [15] and [2] also indicate that rigid impactors may generate initial reaction forces far above the ICAO limits when hitting a typical aluminium aviation mast.

These are strong arguments for the development and the use of a standard soft wing impactor for future frangibility tests. Unfortunately, there is no such standard soft impactor defined as yet, and different variants have been used by mast manufacturers. As a result, the documented crash results [2,5,8,11,13,14,16,18,20,21,22,23] are not directly comparable, neither does the ICAO design manual provide guidelines for soft impactors, or does it restrict the use of data filtering, which has a major impact on the determination of the peak forces [15,4]. The main objective of this paper is, therefore, to document, benchmark and qualify a standard soft impactor design and to propose a prescribed/recommended filtering technique.

The remainder of this paper is organised into sections describing ICAO standards, theory, method, models and sensitivity analysis. The ICAO standard is presented to outline the main design drivers for aviation masts. This section also identifies some contradictions as well as design and test challenges. The theory section addresses the basic modelling and post processing fundamentals applied in the method, and sensitivity sections. The method section documents why and how the various methods are selected in the qualification of the soft impactor. The soft impactor model section presents the NLR wing and its origin, the Beechcraft Model 80 Queen

Air aircraft. A detailed description of the geometry, finite element (FE) models, boundary conditions and loads is also given. The sensitivity analysis section documents how filtering techniques and material model parameter uncertainties influence the soft impactor force and energy curves. Overall, the main research question is to determine whether the addressed model uncertainties can have a critical influence on the ICAO approval of aviation masts, as far as frangibility is concerned.

2. The ICAO standards

2.1. The ICAO frangibility requirements

Figure 1, which is reproduced from Wiggenraad and Zimcik [20], provides an overview of a series of physical crash tests of aviation masts [5,8,14,13,16,22,23] reported in [20], which visualises a major concern about rigid impactors. The impact tests resulting in acceptable damage to the wing sections are bounded by a peak force on the wing of 45 kN, and an energy absorbed by the wing of 55 kNm. These values became the respective maximum values approved by ICAO as design requirements for frangible aviation masts.

As mentioned in Chapter 1, ICAO [17] also recommends the use of a rigid semi-circular impactor in both virtual and physical tests. In this connection, this appears to be a contradiction, since six out of nine test campaigns relate to crash tests with soft impactors. For example,

simulations of a frangible aviation mast provided by Juralco, which was approved by ICAO [15], show that crash tests [14] with a rigid impactor may give initial peak forces far outside these limits. Moreover, the simulation results do not give any indication of the severity of damage caused to a realistic wing since the peak forces are acting in an extremely short-time window.

On the contrary, the pass-fail criterion for the frangibility of the airport masts in Figure 1 was based on actual wing damage. Although skin damage was considered acceptable, the front spar shown in Figure 2 had to survive since it is part of the load carrying structure of the wing, also protecting the fuel tanks. Wiggenraad [18], therefore, concludes that the effect of the wing impactor's rigidity on the impact results should be eliminated from future full scale tests through the use of a standard soft wing impactor. He further states that the impactor damage is the only relevant criterion by which to judge the frangibility of the structure. Here, the relation to actual flight safety aspects is essential and strongly related to the survival of the front spar shown in Figure 2.

2.2. The standard rigid ICAO impactor

The ICAO rules [17] precisely define geometry and material properties of an impactor for full scale test. ICAO recommends the impactor design as a rigid semi-circular tube, with a length of 1000 mm, or five times the

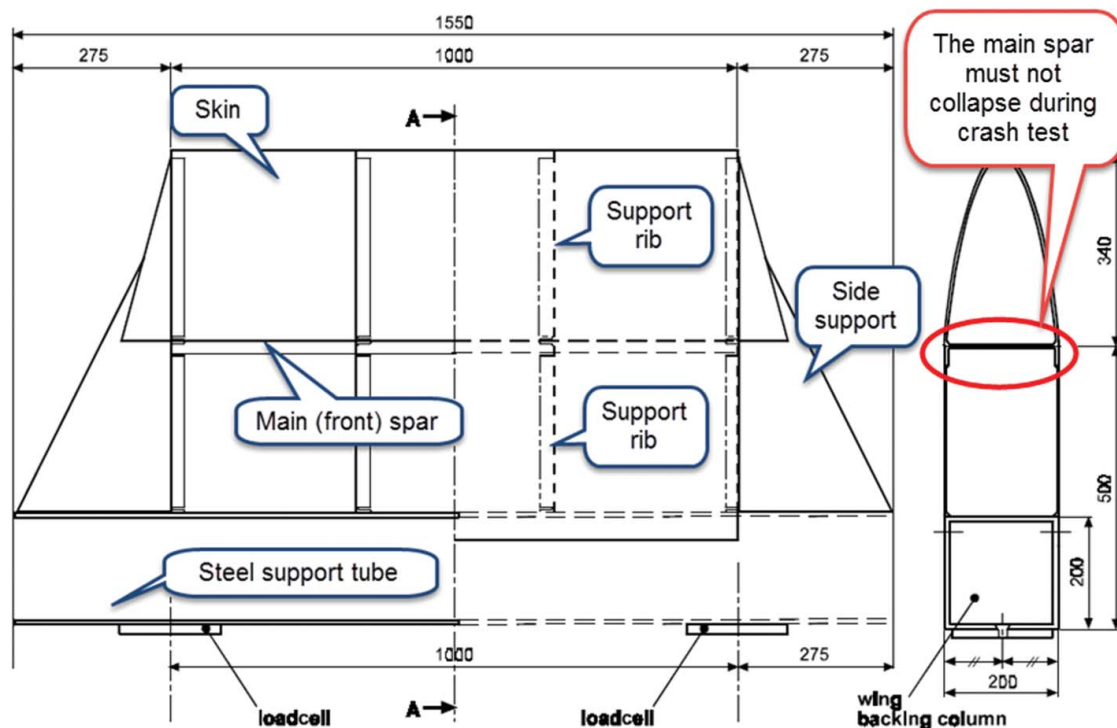


Figure 2. The original NLR soft wing impactor.

maximum cross-sectional dimensions of the tower, whichever is greater. The outer diameter of the tube should be approximately 250 mm and the wall thickness should be sufficiently thick to represent a rigid body but not less than 25 mm. The impactor should have material properties of conventional steel.

2.3. The standard NLR soft impactor model

The intention with the soft impactor, initially proposed by NLR [18], is to use a wing section representative of the Beechcraft Model 80 Queen Air, as seen in Figure 3. This aircraft has a mass of approximately 3000 kg and a take-off speed of approximately 140 km/h. The ICAO standard had adopted these numbers and the soft impactor dimensions and materials are based on this particular airplane.

However, Swedish tests [5,13] referenced in the ICAO standard shown in Figure 1 used a softer non-standard wing impactor based on the Piper PA28 Cherokee. Canadian tests [20,22,23] used both rigid and a soft impactor based on the Piper Aztec, and a version thereof with a thicker wing skin. These references imply that neither the rigid nor most of the soft impactors used in these tests fully comply with the ICAO standard or the proposed NLR design.

The original NLR soft wing design is shown in Figure 2. This figure is identical to the one described by Wiggendaad et al. [18] and used by Robbersmyr et al.

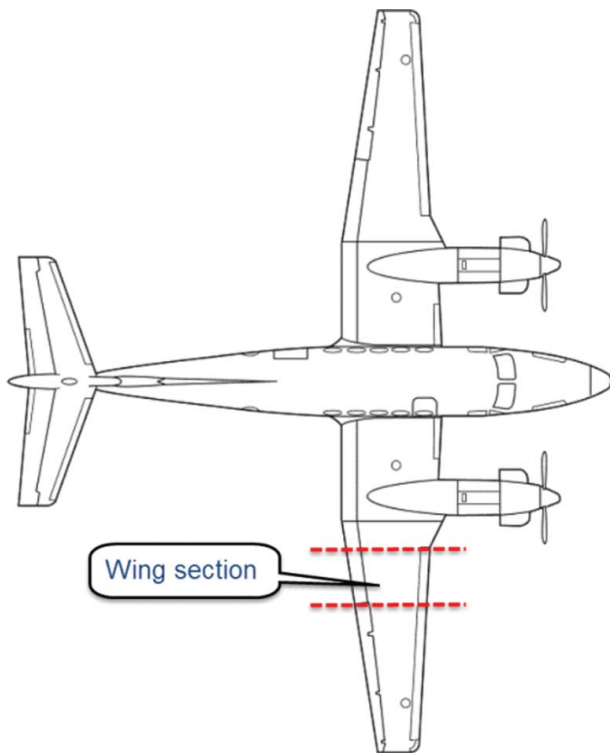


Figure 3. Beechcraft model 80.

[14]. This is the soft wing impactor used in most crash tests and hence the basis on which the ICAO frangibility requirements [9] were established. The material properties are given in [14].

3. Material modelling

The inelastic behaviour of the Alu2024T3 aluminium alloy specified in [12] depends on a number of factors such as alloy composition, upstream processing history, pre-deformation, tempering, etc., making correct modelling extremely complex. In the present study, focus has been placed on investigating the influence of strain hardening behaviour and material's ductility on structural deformation behaviour, including force-deflection characteristic and energy absorption capability, despite the fact that many aluminium alloys may be anisotropic, strain rate and temperature sensitive e.g. under adiabatic heating upon impact. This choice was made from the consideration that the strain hardening behaviour is known to have significant impact on inelastic buckling and subsequent crushing behaviour of metal structures. In addition, strain hardening impacts the formation of necking in uniform uniaxial stretching and a component's ability to redistribute strains locally. The latter is expected to have significant influence on the crushing behaviour of the wing section since it will dictate the transition between crushing type deformation mode and shear fracture type mode. This in combination with lack of a more practical measure of ductility made elongation – obtained in a uniaxial stretching measured as average relative elongation over a certain length usually five times an equivalent diameter of the test specimen – become chosen as the second influential factor in this study. It is well known that the post-necking behaviour, and hence ductility, of aluminium alloys is strongly dependent on a number of other parameters in addition to elongation. In the present study, however, parameters characterising the post-necking portion of the stress-strain curve or any other parameters related to material degradation during plastic deformation have not been considered.

To study the influence of strain hardening behaviour, two different models were applied to represent the Alu2024T3 material [12]. The first one is referred to as a Bi-linear model, which is represented as follows:

$$\sigma = E\varepsilon \quad \text{if } \varepsilon \leq \varepsilon_{0.2} = \frac{\sigma_{0.2}}{E} = 0.0054$$

$$\sigma = \sigma_{0.2} + E_t(\varepsilon - \varepsilon_{0.2}) \quad \text{if } \varepsilon > \varepsilon_{0.2} = \frac{\sigma_{0.2}}{E}$$

Here, $E = 68,563$ MPa is Young's modulus, $\sigma_{0.2} = 367.5$ MPa is 0.2% offset proof stress and $E_t = 470$ MPa

is the inelastic tangent modulus representing the constant slope of the stress-strain curve beyond the elastic limit.

The second alternative is a non-linear model represented by the continuous model established by Ramberg and Osgood (1943), which reads

$$\varepsilon = \varepsilon_e + \varepsilon_p = \frac{\sigma}{E} + k \left(\frac{\sigma}{\sigma_k} \right)^{1/n}$$

in which ε_e and ε_p are the elastic and plastic natural strain, respectively, n is the strain hardening exponent (or parameter), k is the percentage offset and σ_k is the k % offset proof stress. In this case, $k = 0.2\%$, e.g. reference stress is identical with the so-called yield stress commonly used for metals without a well-defined yield point, such as aluminium alloys.

In order to make the two models comparable from a *structural strength perspective* while allowing for the use of readily available material data, both curves were calibrated by directing them through two defined points in the plastic region of the experimental stress-strain curve; i.e. p_1 ($\sigma_{0.2}$, $\varepsilon_{0.2} + 0.002$) and p_2 (σ_u , ε_u). Here, $p_1 = (367.5, 0.0074)$ represents the 0.2 offset proof stress, whereas the second point $p_2 = (625.0, 0.545)$ represents the point on the stress-strain point defining the end of the uniform straining; i.e. the point where the maximum force and elongation occur in a uniaxial tensile test. Here, it should be noted that the location of the intersection point between the two linear regions of the bilinear curve – i.e. the transition from elastic to elastic-plastic behaviour – is slightly different from the defined 0.2 offset proof stress as seen in Figure 4.

Ductility was chosen as the other uncertain material parameter believed to have first-order effect on structural performance of the aviation mast since deformation modes are closely related to this property. Due to the overly complexity of representing material's ductility, the elongation obtained in a standard tensile test (see e.g. ASTM Standard, Designation: E8/E8M–13a) was selected as the ductility parameter for practical purposes. The main argument is that the study concerns identifying uncertainties related to assessing no-go criteria based on aviation mast fragility as seen from the engineering practitioner's point of view, whose access to sophisticated material data and modelling techniques is rather limited. It may also be argued that the strategy of defining a maximum allowable major strain and relate this to a separation cut-off level at single node level in the numerical algorithm may be an oversimplification. Consequently, more sophisticated failure detection strategies – such as evaluating strain differences within a certain path (of elements) or considering stress-strain state or even history – were considered but not applied in the present study.

4. Crash simulation approach

To test the force–displacement characteristics of the standard soft wing impactor, both a static and dynamic simulation approach were selected. The quasi-static compressions tests, which can be verified by less expensive physical tests, were selected as the basis for the sensitivity studies. These compressions tests are expected to give a reasonable estimate of the forces occurring when the impactor hits an aviation mast and deforms until the

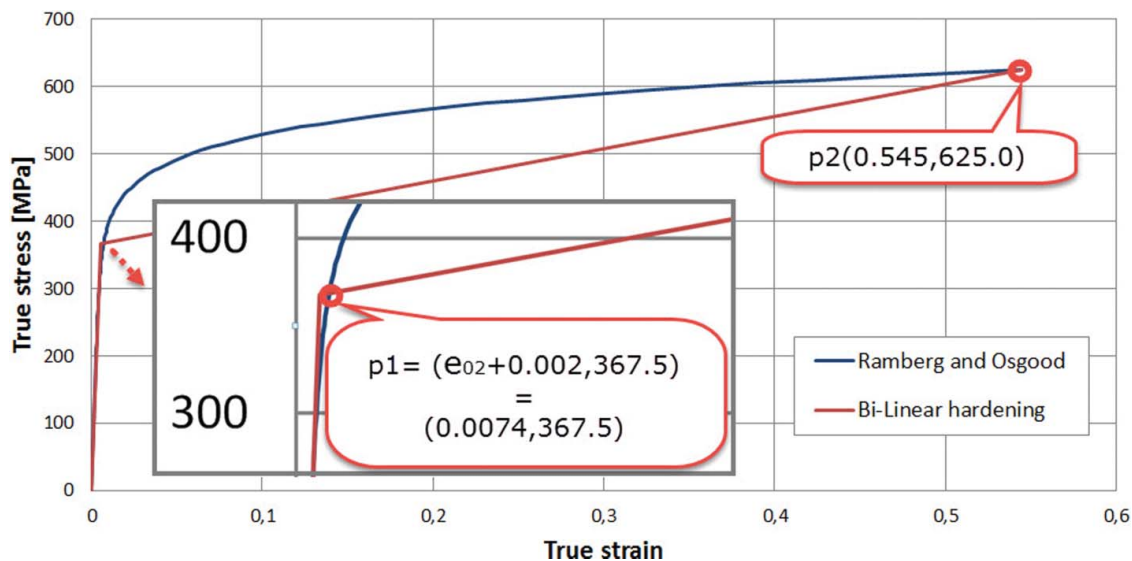


Figure 4. Material hardening models.

main spar and wing collapse. Obviously, the quasi-static compression tests do not consider dynamic effects causing inertia and damping forces. In order to include dynamic reaction and transient peak forces, therefore, additional dynamic crash simulations were performed with an intruder speed of 140 km/h. This is the prescribed ICAO [17] crash test speed. All tests were simulated in Abaqus/Explicit, Version 6.14-1.

5. Filtering techniques

The ICAO rules do not describe the use of data filtering which may have a major impact on the peak forces. Simulations [15] show that the initial peak forces can exceed the ICAO limits when using rigid impactors. However, the duration of these peak forces might be less than 0.2 ms, representing less than 8 mm mast or wing penetration at the given impact speed. An airplane wing section will obviously not collapse catastrophically within 8 mm penetration as the main supporting spar is located 340 mm behind the wing tip. Notwithstanding, the mast will fail to pass the ICAO fragility force criterion.

Although most crash test reports do not document if filtering techniques are applied, the more common practice [8] is to use 1 kHz low pass (LP) (CFC600) filters. The LP filter attenuate frequency components above the specified cut-off frequency (1 kHz) while allowing the low frequency contents to 'pass' through with minimal attenuation. Applied to the above example, 1 kHz LP filtering will eliminate initial and artificial peak forces caused by rigid impactors.

Simulation output requests or sampling rates in physical test measurements are just as critical as the applied filtering techniques. Due to the small time increments utilised in the explicit dynamics integration method, it is common practice to simply request output at some time interval that is much greater than the actual time increment used in the integration algorithm. For noise-sensitive variables, such as impact forces, this approach frequently results in corruption by aliasing as demonstrated in [3].

One fundamental problem in performing crash simulation is not knowing ahead of time the maximum frequency content of the reaction forces. On the contrary, it would be possible to specify a suitable sampling rate capturing the transient dynamics while cancelling the artificial noise.

However, most physical crash tests reported in [18] are using a 10 kHz sampling rate. The time increments used in the crash simulations reported in this paper are typically much smaller (0.1–1 μ s). The simulation output requests were, therefore, set to 10 kHz to match the outputs from physical tests.

Although sampling rate and LP cut-off frequency are not FE model assumptions or uncertainties, they have an a priori unknown influence on the peak forces. Their particular influence on peak forces and hence the approval of aviation mast designs is, therefore, included in this study. The dynamic forces documented in this paper are sampled and plotted at both 10 kHz (output requests) and 1 kHz (after LP filtering). This is common practice in physical crash tests and the corresponding curve plots document how filtering may affect the peak forces.

6. Methods

6.1. Numerical methods and physical testing

The NLR impactor will be used in high-speed virtual and future physical crash testing. The impactor properties should, therefore, be benchmarked by virtual mast intruders hitting the impactor at the recommended ICAO test speed of 140 km/h (38.89 m/s). However, it is not practical to perform physical compression tests of soft impactors at a 140 km/h intrusion speed; i.e. it represents 620 mm compression of a typical dummy mast profile with a cross section of 200 × 200 mm in 0.016 s. The peak forces and accumulated absorbed energy should then be in the range of the specified ICAO limits of 45 kN and 55 kJ. A quasi-static compression test set-up was, therefore, chosen and the (dummy) intrusion speed was set to 50 (mm/min), which agrees with the one previously used in the NLR compression tests [6].

6.2. Explicit versus implicit solver

The choice of static compression tests should presumably favour the Abaqus/Implicit solver. However, it turned soon out the associated contact algorithm could not provide a stable and reliable solution. Both the static and dynamic compression tests were, therefore, run in Abaqus/Explicit, using the general contact algorithm enabling self-contact and a highly non-linear behaviour.

6.3. Energy calculations

The force versus displacement curves could readily be extracted from both virtual (reaction force output request) and physical tests (load cells). The FE method also supports energy plots, yet it is important that the energy curves are calculated by the same suitable method. The absorbed plastic energy curves were, therefore, calculated by integrating the impact forces with the impactor (compression) displacements. The integration

was performed by summing the product of average force and incremental displacement for each time increment.

6.4. Statistical methods

The sensitivity analyses were set up to predict the reaction forces and displacements for all possible variations of input material uncertainties with and without output filtering; i.e. no reduced sample DOF strategy was used. Here, ‘uncertainties’ are regarded as input variations not known or controlled by engineers, e.g. due to material processing variations or lack of common knowledge. More easily controllable and a priori known design parameters like plate thickness, rivet size, dummy mast intruder shape and support structure stiffness are not studied. To reduce the number of the relatively CPU intensive simulations, two material models with different strain-hardening characteristics and three different ‘fracture strains’ (elongation) were tested. Thus, the adopted test strategy addresses the main research question as to how these uncertainties impact the frangibility approval of aviation masts.

7. The Model

7.1. The wing impactor model (CAD/FEM)

The original ‘standard’ NLR soft wing design is shown in Figure 2. This model was the basis for a three-dimensional (3D) model designed in NX9.0 as shown in Figure 5. Taking advantage of symmetry, only a quarter of the full model was created and later mirrored twice. Some simplifications were introduced to simplify meshing and production.

The geometry was idealised in NX Advanced Simulation. The skin ($t = 0.8$ mm), main and nose ribs ($t = 1.6$ mm), side supports ($t = 2.0$ mm) and main front spar

($t = 2.0$ mm) were mid-surface meshed using QUAD4 shell elements with the given thickness. The remaining load cells ($t = 20$ mm) and main support tube ($200 \times 200 \times t = 6$ mm) were mapped meshed with HEX 8 elements. HEX8 elements were selected due to compatibility with the QUAD4 elements and crash solver preferences. The average element size for both solid and shell elements was set to 10 mm, which is expected to be larger than the minimum element size of FE mast models used in crash simulations. The time step set by explicit solvers is limited by among other the minimum element size and material properties based on numerical stability, and the soft impactor mesh should therefore be coarser than the mast’s mesh.

7.2. The ‘dummy mast’ intruder model (CAD/FEM)

To model a realistic compression test set up, a ‘dummy mast intruder’ with the same cross section as the Lattix 4420 aviation mast was selected [1], see Figure 6. This mast model has a typical aviation mast cross section, and is thus expected to generate a realistic reaction force vs. (soft wing) intrusion characteristic. The (dummy) mast cross section has the outer dimensions $197.5 \times 197.5 \times 6.0$ mm. The cross section was extruded 500 mm long, and the 3D solid was assigned to S355J2H steel material properties. The ‘dummy mast’ was mapped (HEX8) meshed in NX as shown in Figure 6.

7.3. The assembly FEM model

The soft wing impactor and mast models were imported from NX as two NASTRAN bulk data files (SI units) and assembled in Abaqus 6.14-1. The HEX8 elements were converted to Abaqus C3D8R hex elements and the QUAD4 elements to Abaqus S4R shells. The bolts and

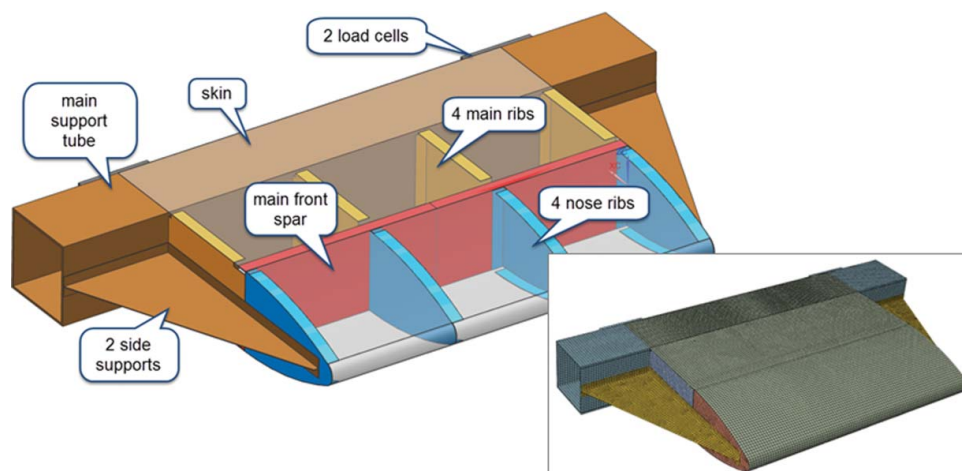


Figure 5. NX CAD/FEM model of the NLR wing.

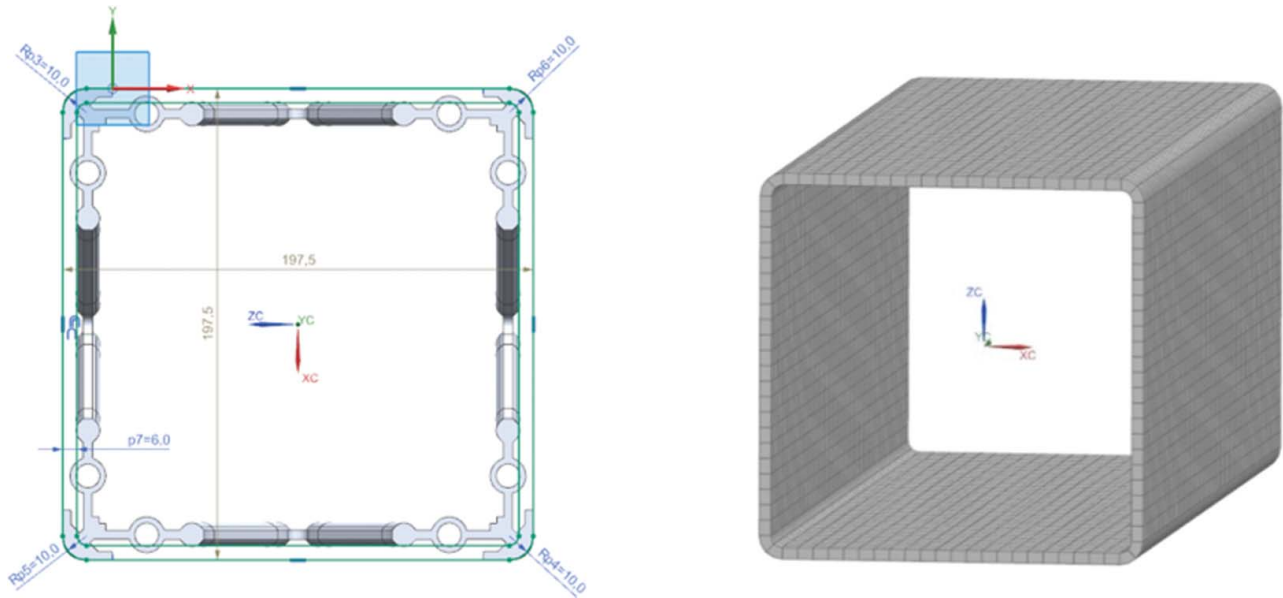


Figure 6. Lattix 4420 and dummy mast cross section (left) and FE model (right).

rivets were modelled in NX as beam elements with circular sections ($D = 6.0$ and 4.0 mm, respectively) since other connector types (rigid elements, springs etc.) are removed from the FE models when used as Abaqus assembly instances. The bolts and rivets were distributed with an average distance of 30 mm. Another advantage with beam elements is that they provide easy change of rivet properties represented by beam sections (diameter) and material data (strain at failure, stiffness, fatigue properties, etc.).

All aluminium rivets and plates (ribs, skin and main spar) were assigned with AA2024-T3 aluminium properties. The other components (side supports, main support tube and bottom support plates) were assigned with standard S355J2H steel properties, as given in Table 1. Loads and boundary conditions are shown in Figure 7.

8. Sensitivity analysis

Two sets of sensitivity compression test were performed. First, an initial compression test was performed to benchmark the model set-up and characterise the deformation modes. Based on the initial test, optimal

Table 1. Material properties.

Property	Material	
	AA2024-T3	S355J2H
Young's modulus (Mpa)	68,563	200,000
Poisson's ratio	0.33	0.3
Yield strength (Mpa)	367.5	355
Ultimate strength (Mpa)	435 @ 10% strain	510 @ 20% strain
Fracture strain (%)	15-25-35	24
Density (kg/m ³)	2700	7850
R&O offset (%): k	0.2	na
R&O strain hardening exponent: n	0.095	na

boundary conditions, solver parameters, output requests, design parameters and uncertainties were identified. These were then applied in static and dynamic sensitivity analysis to study how sensitive the soft impactor wing is to model uncertainties (unknown material properties and filtering).

8.1. Initial compression test

An initial static compression test was run to identify the deformation modes, reaction force and imposed energy versus mast intrusion. A bi-linear material model (elastic-linear plastic) was selected and the fracture strain was set to 15%. Based on the ICAO requirements, the 'soft wing impactor' should survive a max peak load of 45 (kN) and absorbed energy of 55 (kJ) during the compression test. The intrusion (stroke length) was set to 620 mm which is the expected deformable wing

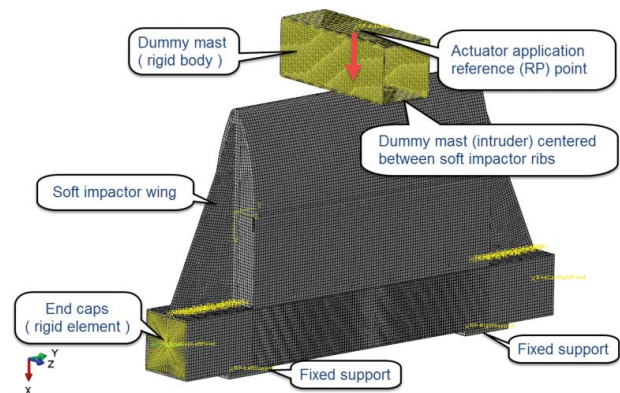


Figure 7. Soft wing impactor compression test set-up.

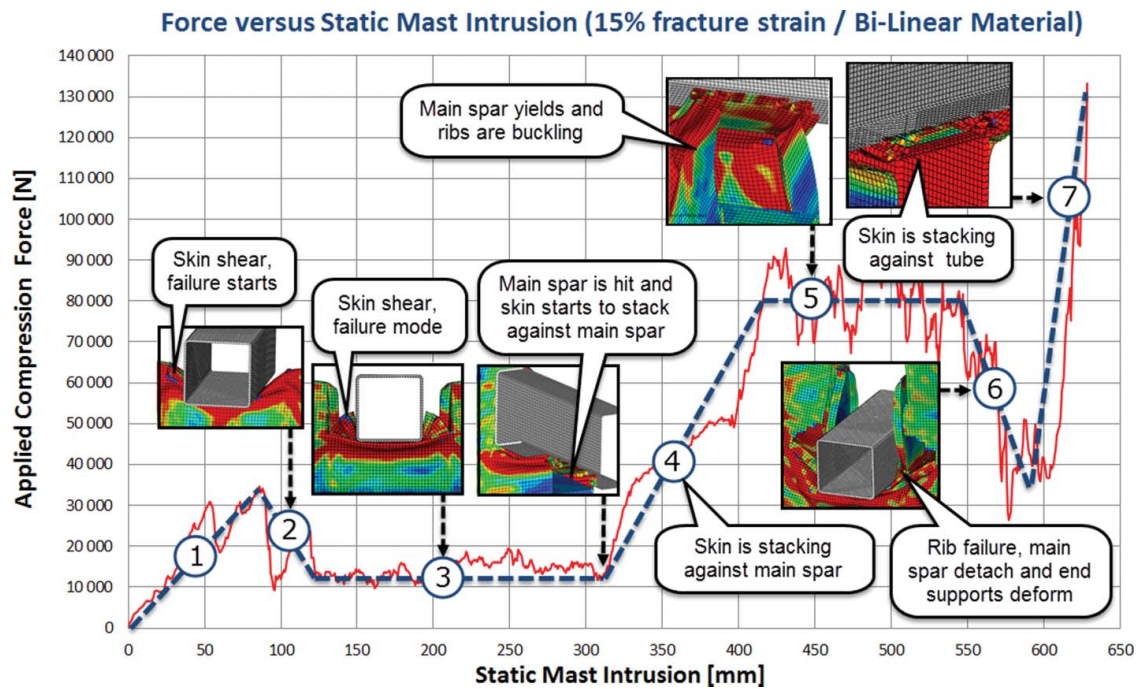


Figure 8. Initial compression test, force versus mast intrusion (intruder stroke).

section measured from the wing tip to the main support tube (see Figure 2). The allowable geometric distance is more than 640 mm, yet the skin will stack up in front of the mast after about 620 mm. It is of key importance that the wing section behaves like a realistic wing and the support structures must not collapse during the test. The steel support tube (Figure 3) shall not deform during the test.

The test was run in Abaqus/Explicit using the general contact algorithm enabling self-contact and a highly non-linear behaviour. The mast was located in the centre of the soft wing impactor (see Figure 7) and the

intrusion speed was set to 50 (mm/min). The AA2024-T3 material is assumed insensitive to strain rate, so the above intrusion speed used in the NLR tests [6] was selected. This quasi-static crushing set-up should presumably favour the Abaqus/Implicit solver, but the associated contact algorithm did not provide a stable and reliable solution. To eliminate large elastic displacements in the 'dummy mast' intruder, the corresponding FEM was defined as a rigid body.

Figures 8 and 9 show the reaction force and energy versus displacement. It can be observed that the reaction force (80–90) is exceeding the ICAO force limit (45 kN)

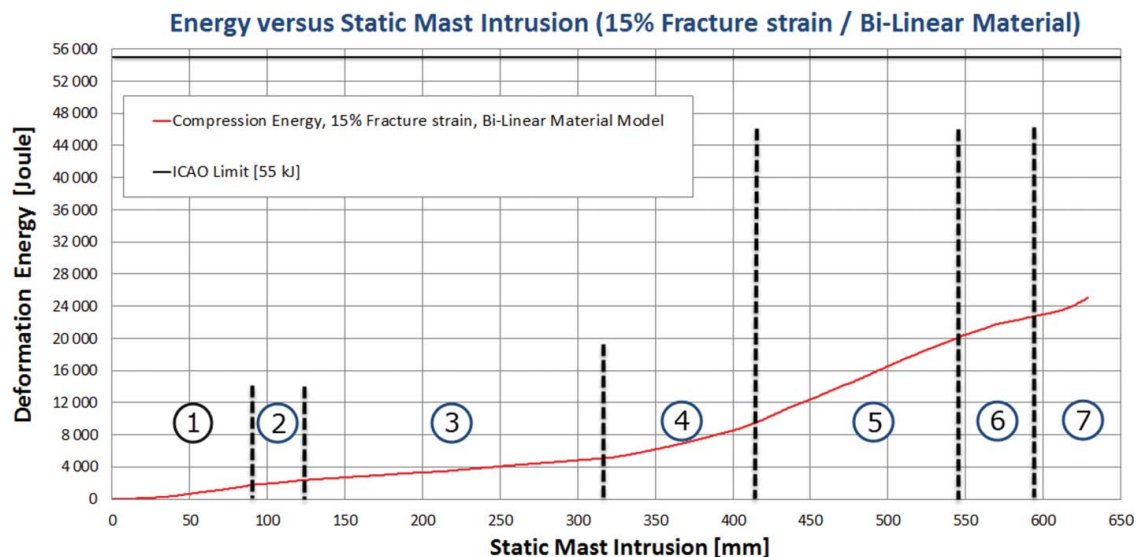


Figure 9. Initial compression test, energy versus mast intrusion (intruder stroke).

Table 2. Soft wing impactor deformation modes.

Mode no	Deformation mode description	Mast intrusion (mm)	Force range (kN)	Energy range (kJ)
1	Linear elastic deformation of skin and main spars	0–80	0–34	0.0–2.0
2	Skin failure (tear open), plastic shear deformation mode	80–120	34–13	2.0–3.0
3	Skin in plastic shear deformation mode, constant force	120–315	13–13	3.0–5.0
4	Skin in plastic shear, stacking up against main spar	315–420	13–80	5.0–9.0
5	Plastic deformation of main spar and buckling of supporting ribs. Side supports start to deform	420–540	80–80	9.0–20.0
6	Rib buckling failure, main spar detach from ribs and skin. End supports are stretched inwards	540–590	80–40	20.0–23.0
7	Skin is stacking up against stiff support tube	590–620	40–130	23.0–25.0

before the main spar collapses, which is an important model feature. These force levels are in the same range as those measured and verified by NLR compression tests [6]. Seven deformation modes were observed during the compression test (Table 2):

The same deformation modes were also observed in the physical compression tests by NLR [6], but the energy level is not optimal. Some undesirable deflections of the side support and main tube did occur in the simulation. In mode (1), the elastic deformation generates a reaction force which peaks at 34 kN before the skin fractures and tears open. Then the reaction force drops to 13 kN when the skin shear mode (2) starts. This wing section deformation behaviour supports the importance of using a soft wing impactor. A rigid body impactor does not deform and generates an almost infinitely high reaction force during initial impact as seen in [15]. This wing impactor gives a reaction force of 34 kN, which is comparable with the test results from [6]. However, sensitivity analyses performed by the author's show that the peak forces are particularly sensitive to rivet size, skin thickness and material properties. There is no definitive answer on how to do this correctly. Mode 3 is similar to the one observed in [6], but the low force level due to tearing (13 kN) gives a minor increase in plastic energy (from 3 kJ to 5 kNm). These results might be sensitive to rivet size, skin thickness and material properties. Mode (4) is dominated by material stacking against the main front spar.

The subsequent deformation modes (5–7) reflect wing collapse and severe flight accidents. Mode (5) is a transition mode from plastic skin shear to buckling-type deformation of the main/front spar and support ribs causing wing failure. This mode must, therefore, be precisely captured by the model and simulation results. In physical tests, visual inspection of the main spar is intended to indicate if the aviation mast is frangible or not. If the spar is broken, the wing has lost its structural integrity and the mast has caused catastrophic damage to the wing and would thus not be approved for use.

When the ribs collapse, however, the modelled side supports seem to be pulled inwards by the main spar. This is not likely to happen with a real airplane

wing since the side supports are a simplified replacement for the aircraft structure. In the sensitivity analysis, the side supports were, therefore, stiffened to match the deformations observed in physical tests [5,8,13,14,16,18,19,23,22]. Mode (6) is dominated by skin and rib buckling failure and finally a major wing impactor collapse. Mode (7) is representing material buckling against the rigid support tube, which gives a dramatic increase in reaction force. The tube is an impactor support not present in a Beechcraft Model 80 airplane wing section.

The above observations mean that the first four 'soft impactor wing' deformation modes are observed in physical tests and hence reasonably well captured by the model and simulation results. On the other hand, mode (5) is the critical mode causing flight accidents and will, therefore, be carefully considered in the sensitivity studies documented in the next section. Modes (6) and (7) are of less practical interest since they only happen when the ICAO force limit is exceeded in mode (5).

The absorbed plastic energy is significantly lower (maximum 25 kJ) than the ICAO requirement (55 kJ). This indicates that the mast will fail the ICAO frangibility force requirement before the energy limit is exceeded. It is noted that these force and energy numbers are in the same range as those measured and verified by NLR compression tests [6].

8.2. Model sensitivity to uncertainties

Based on the initial compression test, the side supports were stiffened and the following material and post-processing uncertainties were identified as listed in Table 3.

The true local strain at fracture (DV1) is to be regarded as an unknown with great influence on the plastic behaviour of an aluminium alloy structure. The fracture strain is dependent on the measuring method and deformation mode (strain state), and it is legitimate to discuss how relevant fracture strain is as a measure of ductility. The soft impactor wing will be heavily compressed/crushed and passes through seven different modes of deformation as shown above. This design variable is expected to have a major impact on the first five first critical modes.

Table 3. Sensitivity to model uncertainties.

Design variable	Model uncertainty	Requirements	
		Range	Expected effect
DV1	Strain at fracture	15%, 25% and 35%	A major influence on absorbed plastic energy and deformation modes (1)–(5)
DV2	Material strain hardening	Bi-linear and non-linear	A major effect on the failure modes and hence both peak force and energy
DV3	Force filtering, cut-off frequency (low pass)	1 and 10 kHz	A major effect on peak forces and hence frangibility approval

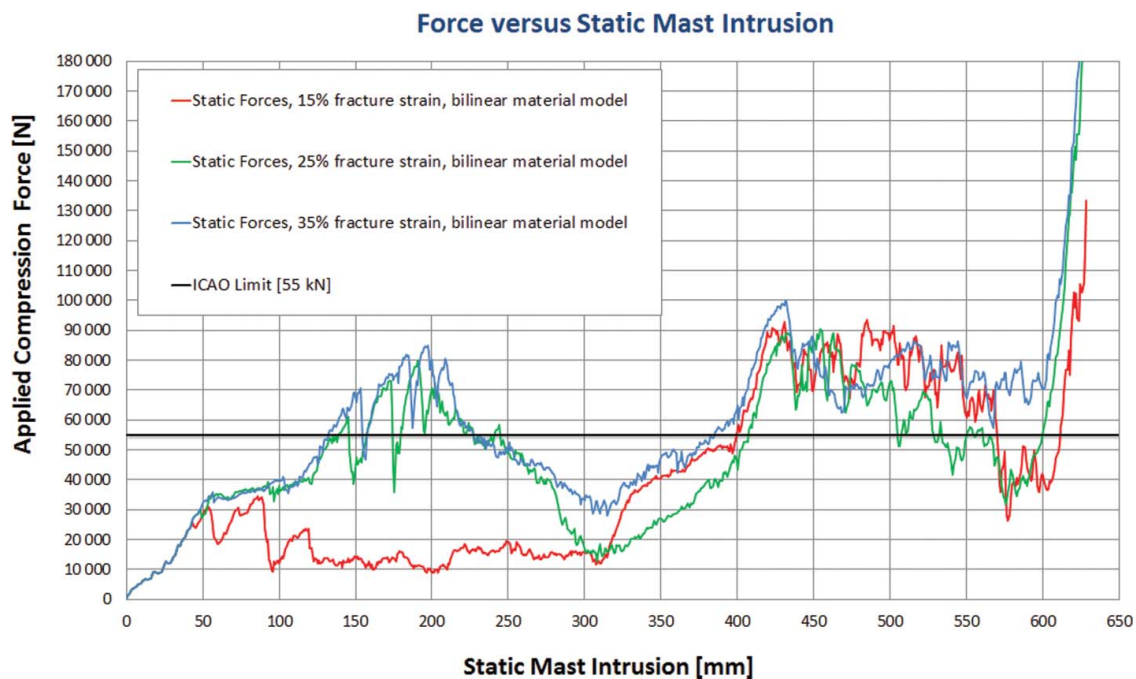
Material strain hardening (DV2) represents the strengthening of a metal by plastic deformation. In non-linear FEA, the strain hardening can be modelled in different ways depending on material, processing and temper condition. It is well known from structural problems that the inelastic portion of the stress strain influences buckling behaviour in case the structure is sufficiently compact. Modelling of the strain hardening characteristic of AA2024-T3 is considered to be a concern – at least when it comes to a common best-practice among structural engineers – representing an uncertainty with significant influence on the failure modes.

Force filtering (DV3) is really not a design variable yet a post-processing feature frequently used to remove noise and artificial peak values from simulation and test data. Based on a literature review of previous physical tests [2,4,5,8,11,13,14,16,18,19,20,21,22,23] and test simulations with rigid impactors [15], the LP filtering of forces and acceleration data is reported to have a major impact on the results and hence aviation mast frangibility.

8.3. Sensitivity to strain at fracture (DV1)

Three different strains at fracture (DV1) values were selected. These were 15%, 25% and 35%, which span the normal range of ductility for AA2024-T3 aluminium, depending on the factors mentioned above. The 15% value used in the initial compression test combined with the Bi-Linear Material model (DV2), gives the seven deformation modes documented in the previous section and shown in Figure 10. When the strain at fracture is increased to 25% and 35%, the skin tear and shear modes are giving much higher reaction forces, exceeding the ICAO limit before the main front spar is hit. The DV1 variations had the same effects on the results when using the non-Linear strain hardening model – however, the forces were generally higher.

Only physical tests of this wing model can confirm the correct deformation sequence. However, the 15% strain at fracture value gives the same seven deformation modes as the ones observed in previous physical tests by NLR [6]. Since the wing main front spar is designed to collapse when the ICAO limit is exceeded, strain at

**Figure 10.** Force versus static mast intrusion (Bi-linear strain hardening).

fracture values above 15% gives too high reaction forces before the skin tears open.

8.4. Sensitivity to strain hardening (DV2)

The two strain hardening material models were tested for the three strains at fracture (DV1) values. With 15% strain at fracture, the non-linear strain hardening model gives higher reaction forces in the skin tear open and shear deformation modes as shown in Figure 11. The bi-linear hardening material model gives a less ductile behaviour and the skin tears open with less initial skin buckling. The non-linear strain hardening seems to delay the skin shear, and buckling has a larger influence on the first three shear deformation modes observed in the initial compression test. The strain hardening characteristic has a minor effect after the skin shear modes are completed and the main front spar is loaded.

When the strain at fracture is increased to 25% and 35%, the strain hardening model has almost no influence on the simulated reaction forces as can be shown in Figures 12 and 13. Compared to the tests performed by NLR (20), a bi-linear strain hardening model seems to give a more correct shear behaviour in deformation modes (2) and (3) (ref. Initial compression test) than the non-linear model. Since NLR used a different dummy intruder and a slightly different impactor wing design, physical tests need to be performed to verify the correct deformation sequence and material model.

8.5. Sensitivity to low pass filtering (DV3)

In order to test LP filtering, dynamic compression tests were performed. An intruder speed of 140 km/h was selected as specified in the ICAO crash test recommendations [17]. Dynamic compression simulations capture the inertia and damping forces absent in the static compression tests and hence the transient dynamic forces that tend to exceed the ICAO limits without filtering.

8.5.1. Dynamic effects on total reaction force and energy

The dynamic compression tests changed the first three deformation modes found in the initial static test as shown in Figure 14. The skin did tear open much earlier and static deformation modes (1) to (3) were more dominated by local shear and rivet failure. The initial peak force after mode (1) was almost the same as in the static test but inertia forces added to the shear forces when the skin material started to stack in front of the high-speed intruder. As a result, the total compression force was oscillating around an almost constant value (20 kN) until the material started to stack up against the steel support tube after 500 mm intrusion. The deformation modes (1) to (3) were not sensitive to fracture strain or material hardening models.

The deformation modes (4) to (6) were more sensitive to both the fracture strain and the hardening model. The loading and failure of the main spar was captured for all material combinations but the peak levels increased with

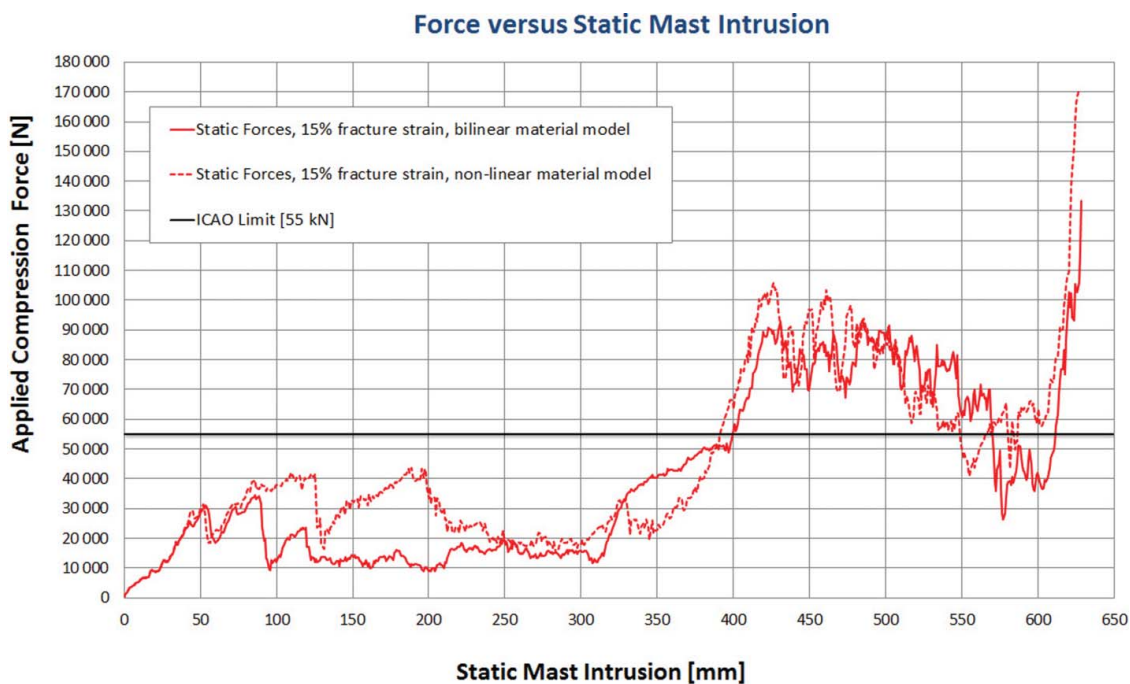


Figure 11. Force versus static mast intrusion (15% strain at fracture).

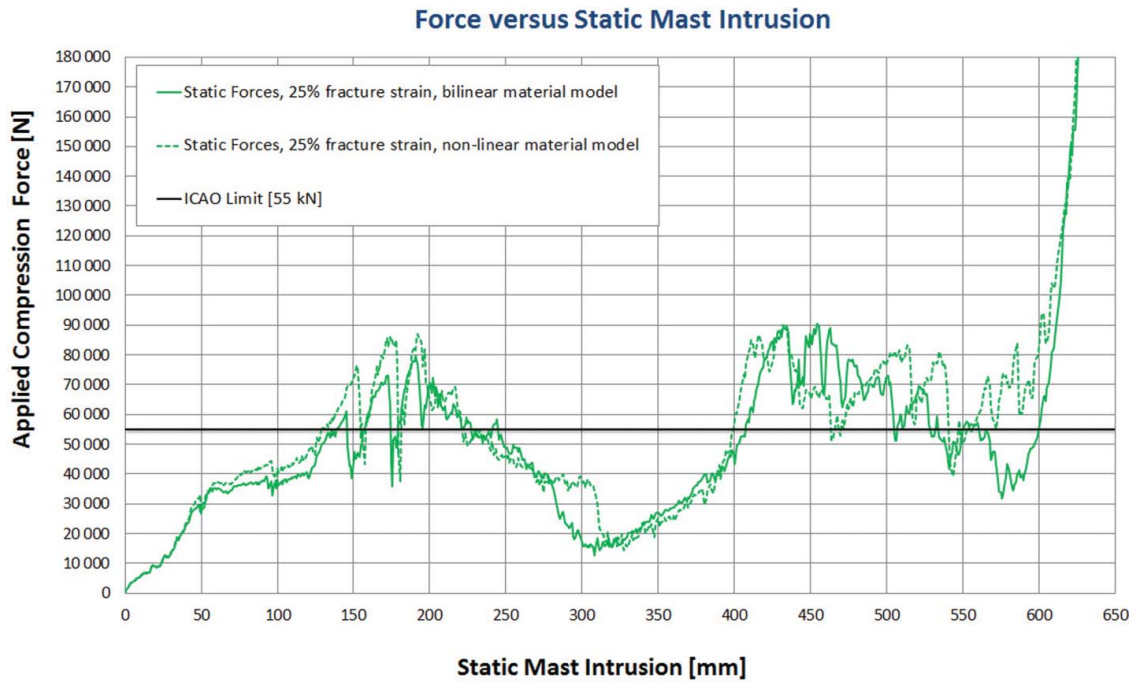


Figure 12. Force versus static mast intrusion (25% strain at fracture).

the strain at fracture values. The dynamic simulations showed that the ICAO force limit was exceeded before the main spar collapsed and the skin started to stack against the rigid support beam. Consequently, it is suggested that visual inspection of the main spar in physical high-speed crash tests can be sufficient to document that the aviation mast is not causing reaction forces above

the ICAO limit. However, the main spar is not collapsing before the peak load is in the range of 100–180 kN, which is far above the ICAO limit.

The accumulated compression energy (based on 10 kHz force and displacement sampling) did only exceed the ICAO limit (45 kNm) for the non-linear material model with 35% strain at fracture (Figure 15).

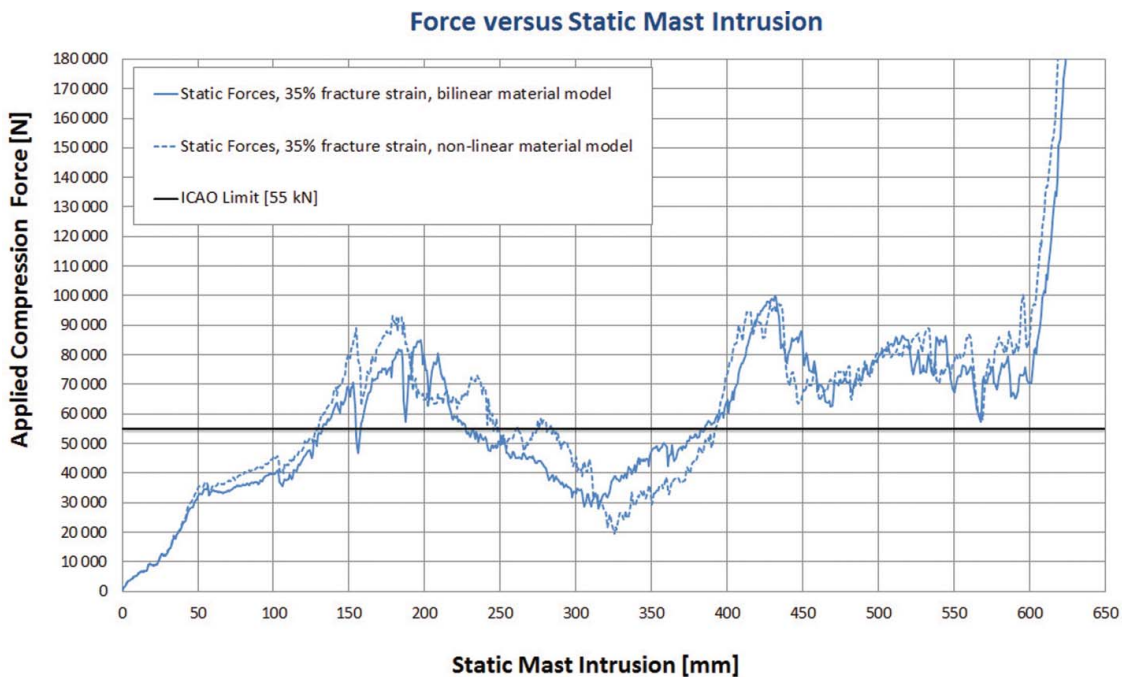


Figure 13. Force versus static mast intrusion (35% strain at fracture).

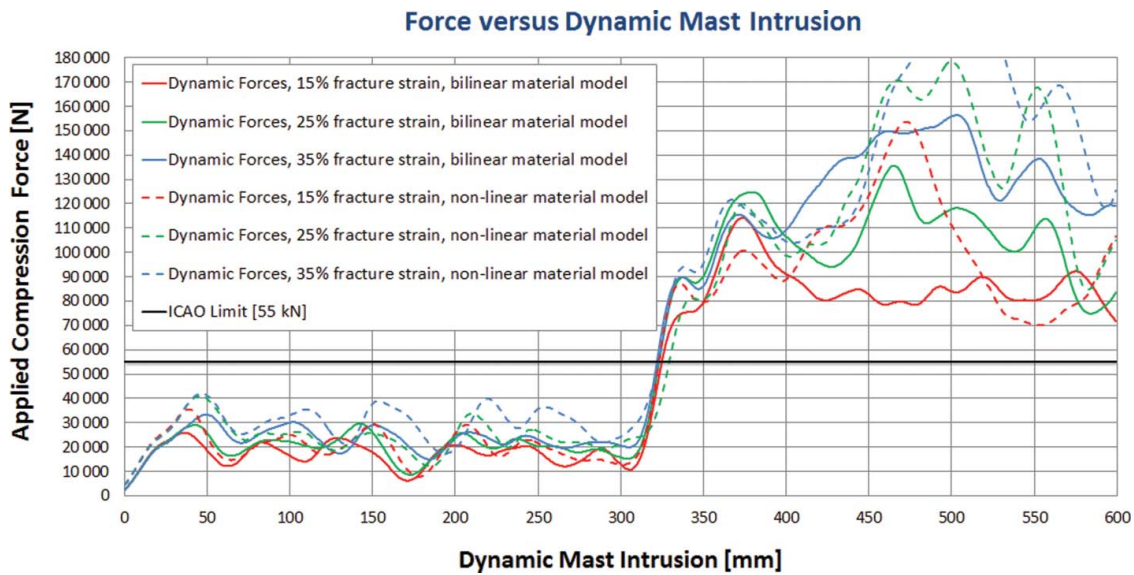


Figure 14. Force versus dynamic mast intrusion (140 km/h, 1 kHz low pass).

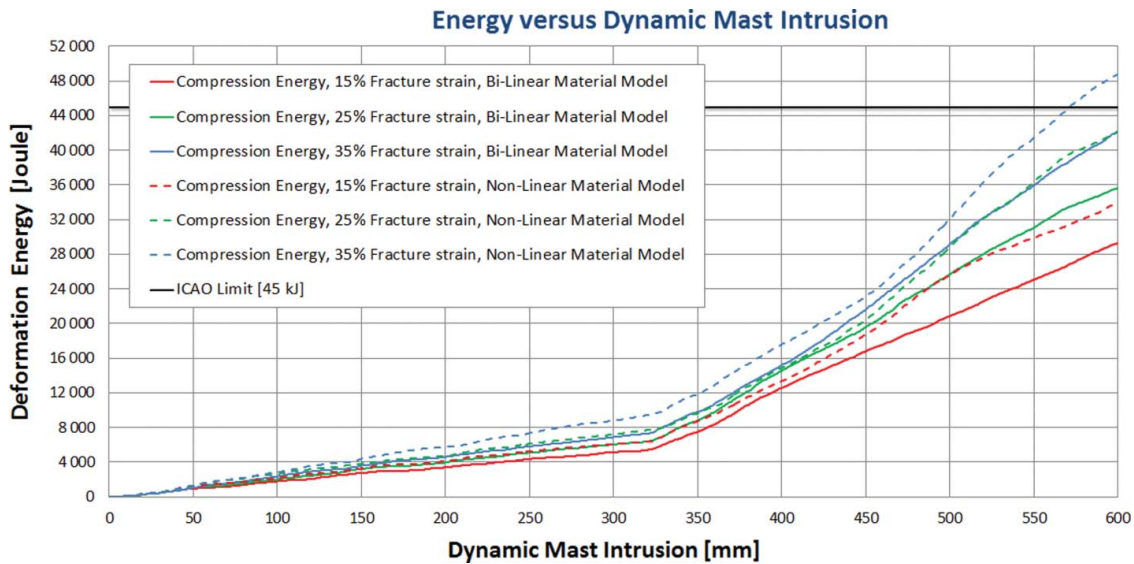


Figure 15. Energy versus dynamic mast intrusion (140 km/h, 1 kHz low pass).

This actually excludes this material combination as realistic since no aviation masts [18] have ever failed the ICAO energy criteria (see Figure 1).

It is hard to benchmark these results, but studies of aircraft wing damages indicate that the combination of 15% fracture strain and the bi-linear hardening model best capture the deformation modes in high-speed

crashes. Higher strain at fracture values (25%–35%) seems to eliminate rivet fractures and shear deformations observed in physical tests [18].

8.5.2. Low pass filtering effects

The LP filtering has a major influence on the peak forces acting in the dynamic simulation. Table 4 shows that the

Table 4. Force sensitivity to low pass filtering.

Strain at fracture (%)	Dynamic Peak forces (N)							
	Bi-Linear strain hardening				Non-linear strain hardening			
	No filter	10 kHz	1 kHz	Peak Reduct. (%)	No filter	10 kHz	1 kHz	Peak Reduct. (%)
15	168,979	127,882	114,141	33	242,017	153,700	187,628	23
25	348,045	210,319	135,631	61	349,785	213,244	178,458	49
35	277,714	189,624	156,398	44	317,149	232,511	210,829	34

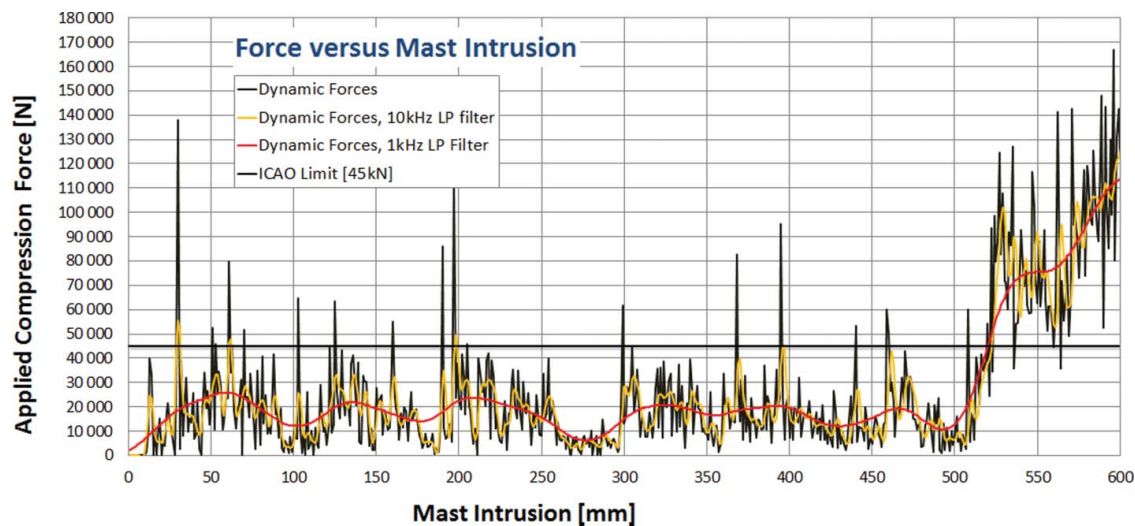


Figure 16. Force versus dynamic mast intrusion (No, 1 kHz, 10 kHz LP filtering).

peak reduction, when applying a commonly used 1 kHz LP filtering, varies between 23% and 61%. Higher reductions are observed for local peak values, though.

The filtering effect is even more obvious when studying Figure 16, showing the unfiltered and filtered dynamic forces (bi-linear material with 15% strain at fracture). If the rigid intruder was replaced by an aviation mast, it would fail the frangibility force criteria after less than 30 mm intrusion. However, when applying a 1 kHz LP filter, the initial and presumably unphysical peak force is reduced from almost 140 kN to approximately 20 kN, which is well below the 45 kN limit. These types of effects are observed when filtering is applied to the force characteristics for all combinations of strain at fracture (DV1) and strain hardening models (DV2).

Table 5 shows that the sample frequency (LP cut-off frequency) has almost no influence on the energy when calculated as the integral of total intruder impact force along the intruder deflection. This confirms that the peak forces in Figure 16 arise within extremely short-time intervals and hence have almost no contribution to the wing impactor damage.

These results indicate that the commonly used 1 kHz LP filtering [2,4,5,8,13,14,16,18,20,21,22,23] eliminates peak forces that have almost no effects on the applied plastic energy (i.e. wing damage). It may, therefore, be questionable to use these peak forces as a measure on

mast frangibility – even if they are above the 45 kN ICAO limit.

9. Discussion

The quasi-static compression tests proved that the material hardening models and strain at fracture had a big impact on the force distribution. A bi-linear hardening model with 15% fracture strain captured the deformation modes previously observed in physical tests performed by NLR [6]. This material model also indicates that visual inspection of the main front wing spar is enough to decide if the ICAO limits are exceeded and a wing collapse is likely to have happened.

When the fracture strain is increased to 25% and 35%, the skin tear open mode is mixed with the skin shear mode due to the increased ductility. The ICAO force limit is, therefore, exceeded before the main spar is damaged. Visual inspection of the main spar is, therefore, not applicable to airport mast frangibility approval if the soft impactor wing material has a fracture strain above 15%.

A non-linear hardening model is less sensitive to the fracture strain, and the force distribution was quite similar for all fracture strain values (15%, 25% and 35%). The skin tear open deformation mode was not identified with 15% fracture strain as for the bi-linear hardening model. The bi-linear hardening model, therefore, gives a better match with the NLR test results. However, 15% fracture strain and the non-linear hardening model do not give force values above the ICAO limit before the main spar is damaged. Visual inspection of the main wing spar is, therefore, applicable as a mast frangibility approval indicator.

Table 5. Energy sensitivity to low pass filtering.

Fracture strain (%)	Compression energy (Nm) (bi-linear strain hardening)	
	10 kHz	1 kHz
15	29,269	29,222
25	35,608	35,623
35	42,132	42,070

For 25% and 35% fracture strain, both the bi-linear and non-linear hardening models gave peak force values above the ICAO limits. Based on the NLR tests, it is, therefore, reasonable to assume that fracture strain values in the range of 15%–25% give more reliable simulation results. This should be verified in physical compression tests since NLR used a different test intruder [6].

The dynamic compression tests introduced inertia loads that changed the deformation modes. The initial skin tear open deformation mode was not observed and the skin shear forces increased due to inertia forces and elastic oscillations. The main spar loading and collapse were captured for all material combinations, but high strain at fracture values (25% and 35%) gave a ductile rivet behaviour not observed in physical tests. Studies of aircraft wing damages indicate that the combination of 15% fracture strain and the bi-linear hardening model best capture the deformation modes in high speed crashes [18].

The dynamic simulations clearly demonstrated the effect of LP filtering of crash simulation results. The peak reduction, when applying a commonly used 1 kHz LP filtering, varies between 23% and 61% and higher reductions are observed for local peak values. These results indicate that the commonly used 1 kHz LP filtering [2,4,5,8,13,14,16,20,21,22,23,18] eliminates peak forces that have almost no effects on the applied plastic energy (i.e. wing damage).

10. Conclusion

The static compression test results were sensitive to both fracture strain and hardening models. Based on previous NLR test results, a strain at fracture value of 15% combined with a bi-linear hardening model gives the most reliable simulation results. This material combination also seems to give the most correct wing impactor behaviour in high-speed crash simulations.

The common 1 kHz LP filtering of reaction forces efficiently eliminates artificial peak forces not contributing to wing damage. The use of LP filtering and the proposed soft impactor wing completely eliminate problems with artificial peak forces that exceed the ICAO frangibility force criteria.

The ICAO energy limit is not sensitive to material models or artificial transient forces. The simulations show that the accumulated deformation energy is far below the ICAO limit even when the force limit is exceeded. However, the ICAO energy limit may be more applicable to the approval of heavier aviation masts with electric cables included in the test set up.

However, these results should be verified by physical compression tests to identify the correct fracture strain and material hardening for the wing impactor. The proposed standard wing impactor is based on the NLR design used in most physical tests. The authors' intention is to establish a benchmark and distribute a FE model of the wing impactor for future crash testing of aviation masts.

Disclosure statement

No potential conflict of interest was reported by the authors.

ORCID

Terje Rølvåg  <http://orcid.org/0000-0003-0677-3154>
Torgeir Welo  <http://orcid.org/0000-0002-0731-9992>

References

- [1] http://www.lattix.net/files/Lattix_Mast_4420_EN.pdf, September 2015
- [2] J. Czujko, *Juralco aviation masts*, Technical Report Doc. NTR-2008-007 – Rev D, Oslo, 2008.
- [3] T. Diehl, D. Carroll, and B. Nagaraj, *Using digital signal processing to significantly improve the interpretation of Abaqus/Explicit results*, Proceedings of ABAQUS Users' Conference, Chester, May 25–28, 1999
- [4] D. Duke, *Airfield frangibility criteria, questions and concerns with current standards*, Presentation at the JAFSG Meeting II at IES ALC in Orlando 24 Oct, Orlando, FL, 2014.
- [5] G. Eriksson, *Horizontal impact tests on approach light masts*, Board of Civil Aviation of Sweden, Report 1985:01/Ue, Norrkoeping, 1985.
- [6] R.H.W.M. Frijns and J.F.M. Wiggenraad, *Static compression tests and computer models of wing impactors used for impacts on frangible airport approach lighting towers*, NLR-CR-99495. Report can be ordered from the authors, Marknesse, 1999.
- [7] B. Griffith, *Frangibility impact testing review*, Presented at the JAFSG meeting in Orlando 24 Oct, Orlando, FL, 2014.
- [8] J. Hanka and M. Vahteri, *Impact tests of EXEL approach light masts*, NESTE, Test Report, 1991.
- [9] International Civil Aviation Organization (ICAO), *Aerodrome design manual*, draft, Part 6, Frangibility, Revised ed.
- [10] JASFG - Joint Airfield Frangibility Study Group, <https://www.linkedin.com/groups?home=&gid=6702609>
- [11] M.A. McCarthy, J.R. Xiao, N. Petrinic, A. Kamoulakos, and V. Melito, *Modelling bird impacts on an aircraft wing – Part 1: Material modelling of the fibre metal laminate leading edge material with continuum damage mechanics*, Int J Crashworthiness 10 (2005), no. 1, pp. 41–49.
- [12] A. Morascha, D. Matiasa, and H. Baier, *Material modelling for crash simulation of thin extruded aluminium sections*, Int J Crashworthiness. 19 (2014), no. 5, pp. 500–513.

- [13] J. Olthof, *Impact testing of full-scale frangible approach lighting structure*, NLR CR-90-239, 1990.
- [14] K.G. Robbersmyr and O.K. Bakken, *Impact Tests for Juralco Lattix Airport Approach Light Towers*, Mechanical Department, Agder College, Kristiansand, 1997.
- [15] T. Rølvåg, *Frangible aviation masts, research questions for my sabbatical year*, Presentation at the JAFSG Meeting II at IES ALC in Orlando 24 Oct, Orlando, FL, 2014.
- [16] E. Sallinen and M. Vahteri, *Horizontal Impact Tests on Airport Approach Light Masts*, Test Report, NESTE, Materials Research Dept., Houston, TX, 1990.
- [17] M.H. van Houten, H. Gottschalk, C. Rooks, R. Miller, and P. Tolke, *International Crashworthiness Conference ICRASH2010*, Leesburg, VA, 2010, 22–24.
- [18] J.F.M. Wiggenraad, *Summary of impact test results for frangible and support structures*, NLR Contract Report CR 92153L, Marknesse, 1992.
- [19] J.F.M. Wiggenraad, A. de Boer and R.H.W.M. Frijs, *Impact simulation of a frangible approach light structure by an aircraft wing section*, NLR-TP-2000-618, Marknesse, 2000.
- [20] J.F.M. Wiggenraad and D.G. Zimcik, *Frangibility of approach lighting structures at airports*, NLR-TP-2001-064, Marknesse, 2001.
- [21] D.G. Zimcik, M. Nejad Ensan, S.T. Jenq, and M.C. Chao, *Finite element analysis simulation of airport approach lighting towers*. *J. Streuct.* 130(2004), pp. 805–811.
- [22] D.G. Zimcik, S.A.Q. Saddiqui, and M.H. Toorani, *Frangibility of airport approach lighting towers, Phase III*, *Transport Canada*, ASIC-E-00-1, WITPress, 2002.
- [23] D.G. Zimcik and A. Selmane, *A study on the frangibility of airport approach lighting towers, Phase II*, *Transport Canada*, ASIC-E-98-1, ASCE, 1998.